1

A Fully Automated Multichannel Digital Electrical Impedance Plethysmograph

Ravi Shankar, Shu Yong Shao and John G Webster

ABSTRACT:

We developed a PC (personal computer)-based 3-channel electrical impedance plethysmograph for automated data collection on human subjects in a clinical validation study. The instrument was driven by a standard PC and was totally transparent in its operation to the medical personnel at the clinical site. The protocol required data collection from three simultaneous channels, over a period of up to 20 min. Continuous use by clinical personnel and repeatable results are evidence of its usefulness.

INTRODUCTION:

A plethysmograph noninvasively measures changes in volume. An electrical impedance plethysmograph uses a 2 or 4-electrode configuration to send a small high-frequency current through a body segment and measures the resulting voltage. The voltage divided by the current yields tissue impedance (Z) and any dynamic changes in it (ΔZ). In turn, these measurements yield change in tissue volume (ΔV), which reflects changes in physiological and/or pathological processes. Plethysmography has been adapted for clinical use on a wide variety of body segments [Webster, 1998]. In our lab, we have used an impedance plethysmograph to acquire noninvasively pulsatile limb segment volume changes as the blood pressure pulse propagates through the blood vessels in that limb segment. The ratio of this volume change to the pulse pressure height causing it yields a measure of the compliance of the artery. We found that the maximal value of this compliance (typically obtained at zero transmural pressure) correlates well with atherosclerotic risk factors [Shankar and Webster, 1991] and the extent of actual disease [Shankar and Bond, 1990]. Since these pilot validation studies, a group of clinical researchers have validated the method by correlating it with MRI data from the abdominal aorta [Harrington et al., 2004]. They used a simplified protocol and volume plethysmography; both reduced the sensitivity of the method. Despite that, they were able to confirm the method's ability to add significantly to the predictive ability of well known cardiovascular risk factors.

This paper describes the first clinical multichannel research instrument that was built to support this study. Data collection with this helped refine the system and develop a simpler instrument and protocol which were used eventually. An impedance plethysmograph, judiciously used, allows one to measure different electrical properties of the underlying tissue and its constituents, since one can vary the frequency, direction of application, the site of measurement, and the number of sites where simultaneous measurements are made. Further, it is noninvasive and relatively simple to use. Our system is designed to be highly reliable and repeatable, and is PC-based so a standardized protocol can be rigorously enforced; real-time and off-line signal processing can be undertaken for further analysis; applied and measured electrical parameters can be varied; and the clinical researchers can use the instrument with no technical help. We only describe the instrumentation here; two other papers will describe the front end (the

protocol implementation) [Shankar, Martinez, and Webster, 2008] and the back end (the digital signal processing algorithms used) [Shankar, Gopinathan, and Webster, 2008]. We expect that our highly automated PC-based system will help other researchers to explore further applications that may not have been possible earlier because of the lack of a complete end-to-end system that allowed them to focus exclusively on the research issues. Examples of potential multichannel applications are: determination of pulse-wave velocity [O'Rourke, Safar, and Dzau, 1993] and the Ankle-Brachial Index, ABI [Hirsch, et al., 2005]. Multichannel recording can use cross-channel information to improve digital signal processing algorithms [Shankar, Gopinathan, and Webster, 2008]. This may yield new applications.

We list here the user requirements of such a system: The ratio of voltage measured across the voltage electrodes, to the current applied through the current electrodes, provides tissue impedance. This tissue impedance typically has a dc component (corresponding to the tissue volume of the body segment), Z, and a superimposed ac component, ΔZ; we call ΔZ the impedance pulse. In limb segments, this impedance pulse is caused by cross-sectional and blood resistivity changes that occur in the blood vessels there as the pressure pulse propagates through the limb segment. The modulation index (ratio of the impedance pulse to the tissue impedance) is as low as 0.1% to 2%. Extraction and magnification of the impedance pulse requires that the dc impedance component be removed. Since noise is magnified with the impedance pulse, it is essential that the initial stages not introduce or allow the noise level to increase. Thus, a clinically viable instrument should be designed to have high signal-to-noise ratio (SNR), low sensitivity to drift and motion artifacts, and rugged functionality. A clinical research instrument, further, will require a large dynamic range, self-tests to ensure proper functionality, linearity, and sensitivity of the instrument. Further considerations are: checks to ensure proper electrode contact; a user-friendly interface to implement the protocol; long (30 min or more) data collection periods; and appropriate signal processing to reduce the data stored and extract relevant parameters. The system also should provide appropriate real-time feedback to the operator about the quality of the recordings. .

Figure 1(a) shows the block diagram of a typical impedance plethysmograph available today. It has a constant current source with a high frequency (50 to 100 kHz) and a low amplitude current (1 to 10 mA peak to peak). This current flows through a reference resistor REF connected in series with the tissue segment to be examined. The signal across REF provides a reference bucking signal to remove the dc component of the tissue signal. Both the reference voltage signal and the tissue voltage signal are demodulated with phase-sensitive demodulators that are fed with the current source as the reference carrier signal (in-phase demodulation extracts the resistive component). The output of the reference demodulator is attenuated, either manually or automatically, to equal the dc component of the tissue signal so the difference signal, the impedance pulse, can be amplified. The demodulators in this design are the main sources of noise. Since bucking is done after demodulation, the noise from the demodulators also gets amplified along with the impedance pulse signal, by the amplifier, thus impacting the potential SNR. Shankar and Webster [1984] designed a system based on this concept. The nulling in their design occurs at low (physiological) frequencies.

Figure 1(b) shows an improved arrangement [Urso, Shankar and Szabo, 1990] in which the signal nulling occurs before demodulation, so noise of the demodulator is not

amplified in the output. This approach, to be user-friendly, requires mechanisms to automatically attenuate the high frequency reference signal (10 to 100 kHz), which is typically harder relative to accomplishing the same at a low frequency as with Figure 1(a). The implementation we present here down-samples to a frequency lower than the carrier frequency so this nulling can be successfully attained automatically. The higher the down sampling, the higher is the noise introduced. Thus, there is an engineering tradeoff to address. We chose a down sampling rate of 10 that allowed us to meet the earlier systems' SNR, while significantly improving upon the dynamic range, bandwidth, and the number of simultaneously recorded channels. Appropriate automatic phase shift compensation was also incorporated, in order to ensure in-phase demodulation to extract the resistive component of the impedance pulse. Improvement in reliability required us to move towards digital solutions, while improved repeatability was obtained with better adherence to the protocol, rejection of spurious signals, and improved signal averaging techniques. The former will be discussed here, while the latter details are provided in two other related papers.

METHOD

We have used mostly digital techniques to improve the SNR and the stability in both the frequency and amplitude of the current source signal. Sensitivity to crosstalk and fluctuations in temperature and power supply are also reduced when the design uses digital circuits. The signal acquired from the subject is an amplitude modulated high-frequency voltage signal which may be calibrated to yield ($Z + \Delta Z$) from the subject, where Z is the tissue impedance and ΔZ is the pulsatile component due mainly to the arterial volume change. The envelope (typical modulation: 0.1% to 2%) of the impedance signal yields the ΔZ signal. We increase the modulation index first by removing up to 95% of the tissue impedance (Z) signal, so the modulation index due to the pulsatile component (ΔZ) is increased substantially (by a factor of 16, from 1.6% to 32%). We then sample the resulting signal at its peaks. This peak sampling eliminates the need for a phase-sensitive demodulator, to obtain a signal that is insensitive to noise and 60 Hz interference [Webster, 1998]. We limit our discussion below to only one channel. Extensions to form a 3 channel system were easy in our implementation because of the modular architecture.

Overview of the Present System

Figure 2 shows the block diagram for the voltage channel. A 10 mA (p-p) constant current source at 50 kHz is passed through the limb segment under test. The signal from the voltage-sensing electrodes on the limb segment is input to the pre-amplifier stage through a transformer (T2). The voltage channel contains stages for preamplification, rectification, nulling, amplification, and peak detection, designed to separate and acquire tissue impedance (Z) and impedance pulses (ΔZ) with the aid of the PC. The resistance of the limb segment typically lies between 10 to 30 Ω.

The pre-amplifier stage consists of an instrumentation amplifier that provides a gain of 10.3 to the signal. The instrumentation amplifier feeds an 8-bit ADC (Analog-to-Digital Converter) via a rectifier. The 8-bit ADC samples the signal in synchrony with

the peaks of the "applied" constant-current sine wave signal [see also Pallas-Areny and Webster, 1993]. The 4 most-significant bits (msbs) of the ADC are fed to the 4 msbs of the 12-bit DAC (Digital-to-Analog Converter). Output of the DAC is subtracted from the output of the rectifier. This removes a major part of the carrier signal before further amplification. This has the effect of enhancing the modulation index by a factor of 16. The output of the subtractor is passed to a 16-bit ADC via an amplifier (that provides a gain of 15.8) and a peak detector. The output of the 16-bit ADC is sampled with a signal which is synchronized to the peak of the applied sine wave current source. This signal is passed to the personal computer (PC) for further processing.

The graphs in Figure 2 are illustrative only and depict an amplitude modulated carrier, with the carrier frequency 5 times the modulating frequency. In reality, the carrier frequency is 50 kHz, while the modulating signal has a bandwidth of 0 to 100 Hz, a 500 fold difference. We assume a modulation index of 2%, the expected highest value. As the graphs show, the 2% amplitude modulation is not visually apparent; but once the nulling occurs, with the tissue impedance signal reduced by about 95%, the modulation increases to 32%, which does become visually apparent.

Constant Current Source

A 50 kHz constant-current sine wave is used as the current source signal. We used digital methods to generate this signal as shown in Figure 3. A 7-bit counter is driven by a 5 MHz source (a 40 MHz crystal oscillator through a Divide-by-8 counter) and generates one hundred sequential addresses to scan a ROM address page. We defined a page as 128 words of 12-bit length; only the top 100 words are used in generation of the current waveform. The choice of frequency of the source depends on the application.

ROM Lookup Table: One hundred 12-bit binary numbers representing a whole cycle of a sine wave are programmed into the ROM. The two most-significant bits of the ROM address bus switch between ROM memory pages, where sine waves of slightly different amplitudes are programmed in. This is useful for self-test of the system, as described below. To reduce transient noise, the 12-bit output is latched before feeding to a 12-bit Digital-to-Analog Converter (DAC). The DAC output is low-pass filtered at 300 kHz. This 50 kHz signal is fed to a voltage-to-current (V/I) converter to yield a constant current source. Transformer T1 (3:1) sets the current in the tissue to 10 mA (p-p) (Figure 2).

Synchronization and phase shift adjustment: The acquired impedance signal is sampled in synchrony with the peak of the applied constant current. This is obtained by using the ROM address lines and generating the synchronizing signal with the aid of an address decoder (Figure 3). The address decoder detects the address for the positive peak of the sine wave output current applied to the subject. The peak of the resistive component of the impedance signal would theoretically occur at the same instant. However, there are propagation delays between the ROM in the constant current generation stage and the ADCs that measure the impedance signal. To compensate for these delays, the decoder address input does not correspond to the peak, but to a higher value that accounts for the length of the system's propagation delays. The decoder provides the synchronization signals for ADCs. The Timer was added to overcome instrumentation induced jumps in the output, as discussed below. Multiple ROM pages encode sine waves of different phase shifts, so for the same scanning addresses, current

sources with different phase shifts can be generated. The phase shift is with respect to the applied ROM address. This provides for a PC-based flexible solution to compensate for phase shifts that may vary among the individual subject-visits. The ROM page with different phase shifts (one of 16) is selected under PC control.

Additional Considerations:

(a) Instrumentation-induced Jump: Nulling with the aid of four msbs of the 8-bit ADC may cause jumps in the output. This occurs when a carry or a borrow propagates from/to the 5^{th} bit. Several software and hardware mechanisms can be used to overcome this. We use a 3 s timer in the current implementation (Figure 2), based on requirements of our automated DSP algorithm. Despite this timer, occasional jumps were observed, possibly due to the ADC used. To overcome this problem, we incorporated a jump removal stage in the pre-DSP processing.

(b) Phase Shift Compensation for Peak Sampling: The sine wave of the current source acquires phase shift between the ROM and the signal input to the tissue segment under examination. Sampling synchronized to the peak of the ROM-generated current source signal would not track the peak of the voltage signal. This problem is compounded by the fact that different subjects have different degrees of phase shifts. We determine in real-time the appropriate subject-dependent phase shift so the sampling occurs at the peak of the acquired voltage signal.

We store 16 different phase shifts in the range of –43.2° to 10.8°, with a resolution of 3.6°. During the initial set up, phase shift is determined once all the electrodes have been connected to the patient. For this, we generate two constant current sources at phase shifts of –36° and 0°. The ratio of the impedances (Z values) obtained yield the phase shift needed for the given patient-visit. Once the phase shift has been determined by the PC, the PC drives 4 address lines with an appropriate address to select one of the 16 pages with different phase shifts (4 of the 6 lines from PC – see Figure 3). Figure 3 shows 2 other ROM address lines from the PC. They are used to select different signal amplitudes and are used in the system self-test procedure. See below.

Measurement of phase shifts: (1) Instrumentation Phase Shift: When the external resistor network is used instead of the subject, it was noted that there is a phase shift of about 14.4° between the output sine wave of the ROM and the input sine wave to the 8-bit ADC. (This is due to the various circuits of the instrumentation). (2) Subject Phase Shift: When a subject is tested using the our instrument, there was a greater phase shift (32.4°) between the output of the ROM and the input of the 8-bit ADC than in the case of the resistor network. This additional phase shift (of about 18°) is caused by the electrode and tissue impedances of the subject. Control Signals ADWR., LATCH, and SAMP are accordingly phase shifted with respect to each other. The 3-to-8 decoders from the 7-bit address lines of the ROM generate these signals. See Figure 3.

(c) PC Acquisition of the Tissue Impedance (Z) and the Impedance Pulse (ΔZ): Control signals from the PC are decoded to obtain GETZ and GETΔZ signals for the channel board (see Figure 2). Sampling is done at 5 kHz rate, effectively reducing the PC-acquisition rate from 50 kHz to 5 kHz.

(d) Self-Test and Self-Calibration: These are performed as part of the protocol under the control of the PC. They provide real-time feedback to the medical operator/subject using our PC-based instrumentation.

1. Test for Poor Electrical Contact of Voltage Electrodes: The PC is used to switch in a low resistance of 1 kΩ across the tissue. See Figure 2. If the electrode contact is bad, the electrode contact impedance will be much higher than 1 kΩ. A significantly lower voltage is noted at the channel input when the 1 kΩ is switched in. The PC performs this test on a regular basis during the data collection.

2. Test for Poor Electrical Contact of Current Electrodes: A comparator is used to test for this. When there is good contact, voltage across the primary of the current transformer (see Figure 3) is low. It will go high when contact is poor. The comparator is fed this voltage after rectification and filtering. The comparator output may be read by the PC at any time during the data collection.

3. System Self-Test: Self-test is needed to increase reliability of the values of Z and ΔZ from the subject. We provide an internal resistor in the instrumentation for this purpose. A signal from PC controls the pertinent relay. This relay connects the channel to either this internal resistor or the subject. Voltage is acquired from this internal resistor during system self test. The signal collected is rectified, and sent to the 8-bit ADC in the instrumentation (Z), then peak-sampled for removal of the carrier and amplified to be sent to the 16-bit ADC (ΔZ). Z and ΔZ are thus collected for the channel board. This is performed for 4 different sine waves (with different amplitudes of 100%, 99.9%, 99%, 98%) selected by 2 address lines of the ROM bus (Figure 3). Comparison with preset values validate linearity and sensitivity of the voltage channel. Note: In effect, there are 64 pages of 128 bytes in the ROM; 16 (one each for the 16 different phase shifts) pages for each of the four amplitudes cited above.

4. Noise Reduction and Motion Artifacts: We have addressed these issues in our earlier papers.

RESULTS

The total gain, from the block diagram in Figure 2 is $3 \times 10.3 \times 15.8 = 488$. Assume that the impedance pulse is 0.1% of the tissue impedance Z (say 10 Ω); i.e., $\Delta Z = 10$ mΩ. A current with a 5 mA peak will yield a 50 μV input to the single channel. Hence, the input to the 16-bit ADC equals 50 μV × 488 = 24.411 mV. The corresponding binary count at the output of the 16-bit ADC (±5 V swing) is $(2^{15}/5000) \times 24.411 = 159$. Hence, the computed sensitivity is 15.9 digit counts/mΩ. The actual sensitivity obtained was 12.7 to 13.0 digit counts/mΩ for the three channels. Channel characteristics are determined off-line (prior to shipping) with a resistance network (Shankar and Webster, 1984). Table 1 provides the specifications of our system.

Three 3-channel Vasograms have been built and delivered. Two of them have been used at conferences to collect data on subjects. The third one has worked reliably for over 9 months at the Bowman Gray School of Medicine, Winston-Salem, NC, where data on approximately 100 subjects were collected. We have been able to satisfactorily process the data on 30 of these subjects, indicating the reliability and repeatability of the

instrument. Details on the DSP algorithms and the Repeatability studies will be provided in two other papers.

The system automatically records a set of calibration measures for each subject. They are helpful in validating the data later on, and in ensuring quality of data collection. These include: ΔZ Calibration, Z Calibration, Phase Shift for Self-Calibration, and Phase Shift for Subject. To this, we manually add the following: Number of Voltage Electrode replacements, Number of Current Electrode replacements, and Operator Comments.

Trend analysis

This is performed with a set of expert rules to ensure that the data collected are acceptable. We list them below. Rules 1 to 4 have very tight constraints. This is indicative of the high degree of reliability and repeatability of our system. The last three rules monitor for situations that could lead to less reliable data collection. The results of all these rules are useful in the interpretation of the DSP-averaged data by the experts.

- Rule 1 (Sensitivity): Using the *.sen* file, calculate the averages of the first ten subjects' (00000FB to 00000FL) Z sensitivity and ΔZ sensitivity values for left arm, left thigh and left calf. Use these numbers as the standard values. For each new subject, calculate the difference between the standard and the new values. The percent change should be less than ±1%. If out of range, stop processing and check the logfile for clues. Initiate corrective action.
- Rule 2 (Phase Shift): The phase shift number should be between 2 and 4. If out of range, check the subject's data file for dry skin (*.dat*). If everything is OK, go to the next step.
- Rule 3 (Pressure Control) – This is skipped here as it is beyond the scope of this paper.
- Rule 4 (Impedance): The Z value of the channel between measurement 1 (M1) and 2 (M2) on the same limb segment should be less than ±2 digital (binary) count (or ±0.25 Ω). If not, record this in the *.fla* file.
- Rule 5 (Operator): Check the *fail* and *rep* (replace) electrode flags in the log file (*.log*). They should be zero. If the flags for a given operator are often nonzero, this operator needs to improve his or her performance.
- Rule 6 (Jump Information): Check the *.jmt* file to see if there are any jumps in the measurement and auxiliary channels. If jumps are found, record this in the *.fla* file.
- Rule 7 (Subject Information): Set a Motion Artifact flag in the *.fla* file, if appropriate.

DISCUSSION

The discussion focuses on various issues related to the acquisition of the impedance pulse signal. Several simulations and/or analyses were performed to lead up to appropriate conclusions.

Effectiveness of Peak Sampling: If we were to sample at the carrier frequency rate at the peaks of the carrier signal, the low-pass-filtered signal (filtered to remove the carrier frequency and pass only the modulating signal) would yield an ideal demodulated

signal, if the sampling process were jitter-free. (An analog phase sensitive demodulator, working essentially on the same principle, actually causes a lot more noise because of the nonlinear and nonideal characteristics.) However, sampling at a higher frequency also means storage of a large number of data points, and also the data acquisition boards available at a reasonable price may not support this. We thus chose a sampling frequency of 5 kHz, causing an increase in noise by a factor of $\sqrt{50/5} \approx 3.1$. However, this is substantially better than for the theoretical minimum sampling frequency we could have chosen ($2fm$, where fm is the maximum modulating frequency). We take fm as 100 Hz for the impedance pulse, resulting in a reduction of the noise by a factor of 5.

Optimization of Peak Sampling Frequency: We chose to use 5 kHz because of the reasons given above. Unfortunately, the C routines provided along with the NIDAQ board did not support this sampling rate. We had to rewrite programs in assembly language to obtain this sampling rate. After all the data are collected, we subject the data to pre-DSP processing. We average down to 1 kHz during this phase, subsequent to the application of a jump removal algorithm. We did not want to reduce the sampling rate further because of noise considerations. Our DSP algorithms are optimized for a 1 ms sampling interval [Shankar, Gopinathan, and Webster, 2008].

Effect of Noise Due To Power Line Interference: To study this, we added a 60 Hz signal to an equation representing the amplitude modulation of our instrument. We simulated different degrees of interference to the amplitude modulated signal and simulated the effect of such interference on demodulation by peak sampling. Results show that the SNR gets worse with 60 Hz noise, as expected. Thus, a better 60 Hz reduction technique was required. In ideal phase-sensitive demodulation, 60 Hz noise gets suppressed. In our case, we high-pass-filtered (in the DSP stage) at 1 kHz, which effectively suppressed the 60 Hz. We also chose an instrumentation amplifier with a high CMRR (Common Mode Rejection Ratio).

Effect of Jitter in Sampling: To study this, we introduced both fixed timing errors and random timing errors to the instant of peak sampling, with a maximum jitter of one-thousandth (0.1%) the sampling period Thus, for a sampling frequency of 12 kHz, a jitter maximum of $(1/1000) \times (1/12 \times 1000) = 0.083$ μs was chosen. For 1.2 kHz, the jitter chosen, accordingly, was 0.83 μs. We obtained results for both frequencies at a modulation index of 1%. The conclusion was that a fixed timing error only causes an amplitude change, while random timing errors may cause substantial noise. We reduced the effect of jitter by introducing a peak sampling stage prior to the 16-bit ADC.

Gain, Phase Shift and Voltage Swings: A fixed timing error causes a reduction in the amplitude. We have compensated for this by a combination of hardware and software techniques.

CONCLUSION

We have built a three-channel impedance plethysmograph which uses a combination of analog and digital techniques to lead to a highly sensitive, reliable and repeatable instrument with low noise characteristics. This forms the data acquisition unit that is well integrated with a PC-based protocol front end and an off-line DSP unit at the backend. It has been used successfully by medical/clinical personnel with no prior experience with

such instrumentation. Comparison with other recent publications on such instrumentation shows the significant superiority and originality of our system.

REFERENCES

Harrington, D.K., Brown, W.V., Mosca, L., Davis, W., Eggleston, B., Hundley, W.G., and Raines, J., Relationship Between Arterial Stiffness and Subclinical Aortic Atherosclerosis, Circulation, 110, 2004, pp. 432-437

Hirsch, A.T., Haskal, Z.J., Hertzer, N.R., and others, Writing Committee Members, ACC/AHA Practice Guidelines for the Management of Patients with Peripheral Arterial Disease, American College of Cardiology and American Heart Association, www.acc.org, pp. 1-192, 2005

O'Rourke, M. F., Safar, M.E., and Dzau, V.J., Arterial Vasodilation, Mechanisms and Therapy, Lea and Febiger, Philadelphia, PA, 1993

Pallas-Areny, R., Webster, J.G., Biolectric Impedance Measurements Using Synchronous Sampling, IEEE Trans. Biomed. Eng., BME-40 (8), August 1993, pp. 824-829

Shankar, T.M.R., and Webster, J.G., Design of An Automatically Balancing Electrical Impedance Plethysmograph, J. Clin. Eng., 9 (2), April 1984, pp. 129-???

Shankar, T.M.R., and Bond, M. G., Correlation of Noninvasive Arterial Compliance with Anatomic Pathology of Atherosclerotic Nonhuman Primates, Atherosclerosis, 85, December 1990, pp. 37-46

Shankar, T.M.R., and Webster, J.G., Noninvasive Measurement of Compliance of Human Leg Arteries, IEEE Trans. Biomed. Eng., BME-38 (1), January 1991, pp. 62-67

Shankar, R., Gopinathan, M., and Webster, J.G., Digital Signal Processing in Clinical Validation Studies with Impedance Plethysmography, In preparation, 2008

Shankar, R., Martinez, M., and Webster, J.G., Software Protocol Techniques for Clinical Validation Studies with Impedance Plethysmography, In preparation, 2008

Urso, A., Shankar, R., Szabo, B., Wagner, W.D., Design of a High Signal to Noise Ratio Electrical Impedance Plethysmograph, Proc. IEEE Southeastcon, New Orleans, April 1990, pp. 1100-1104

Webster, J.G., Editor, Medical Instrumentation: Application and Design, 3rd Edition, John Wiley and Sons, New York, NY, 1998

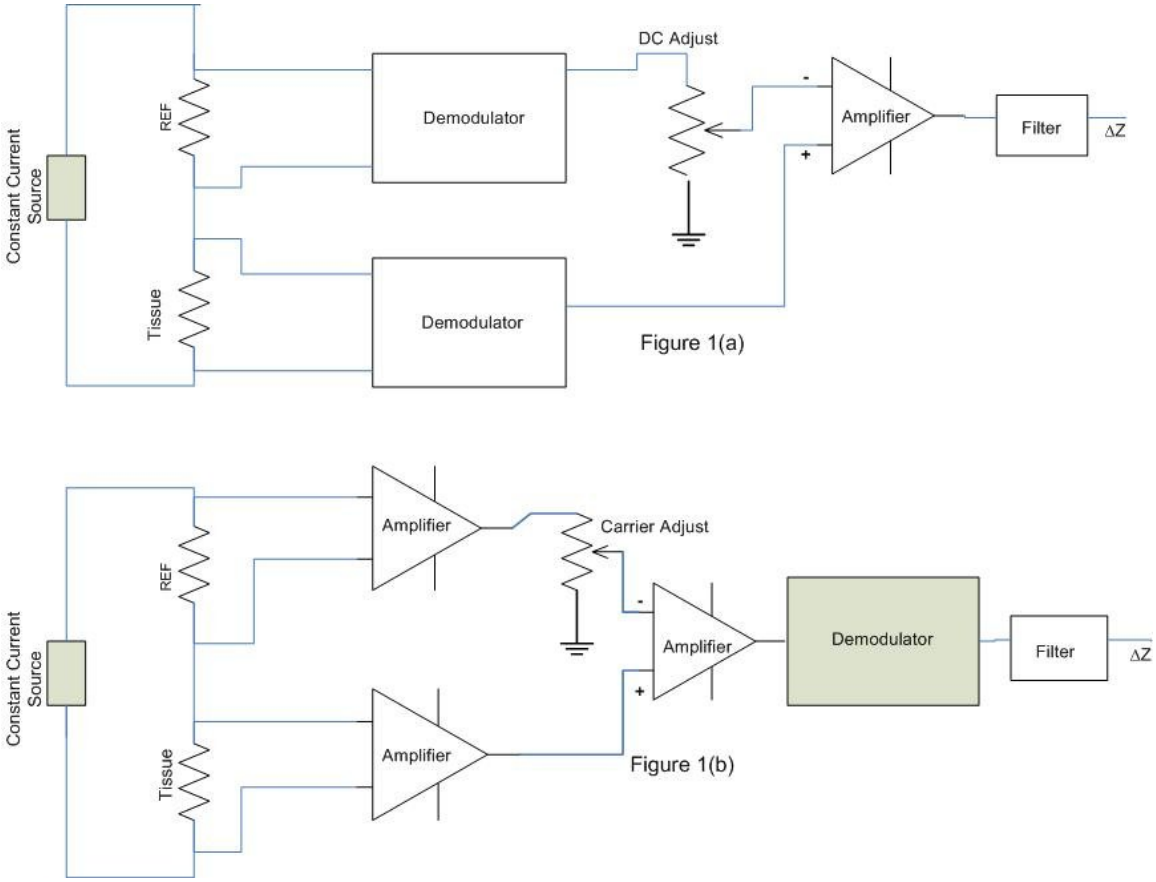

Figure 1: Alternative Ways of Designing an Electrical Impedance Plethysmograph

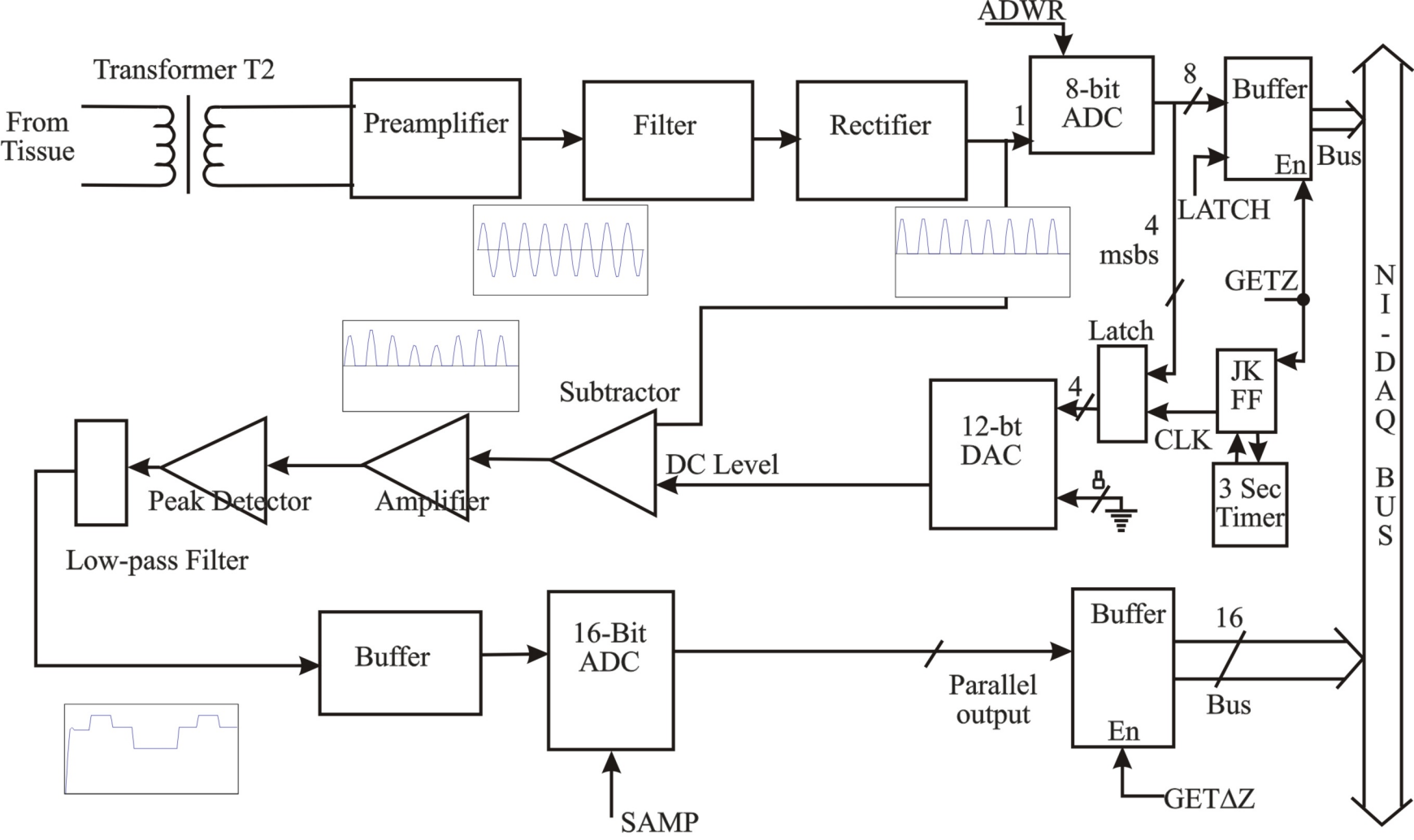

Figure 2: Block Diagram of the Voltage Channel

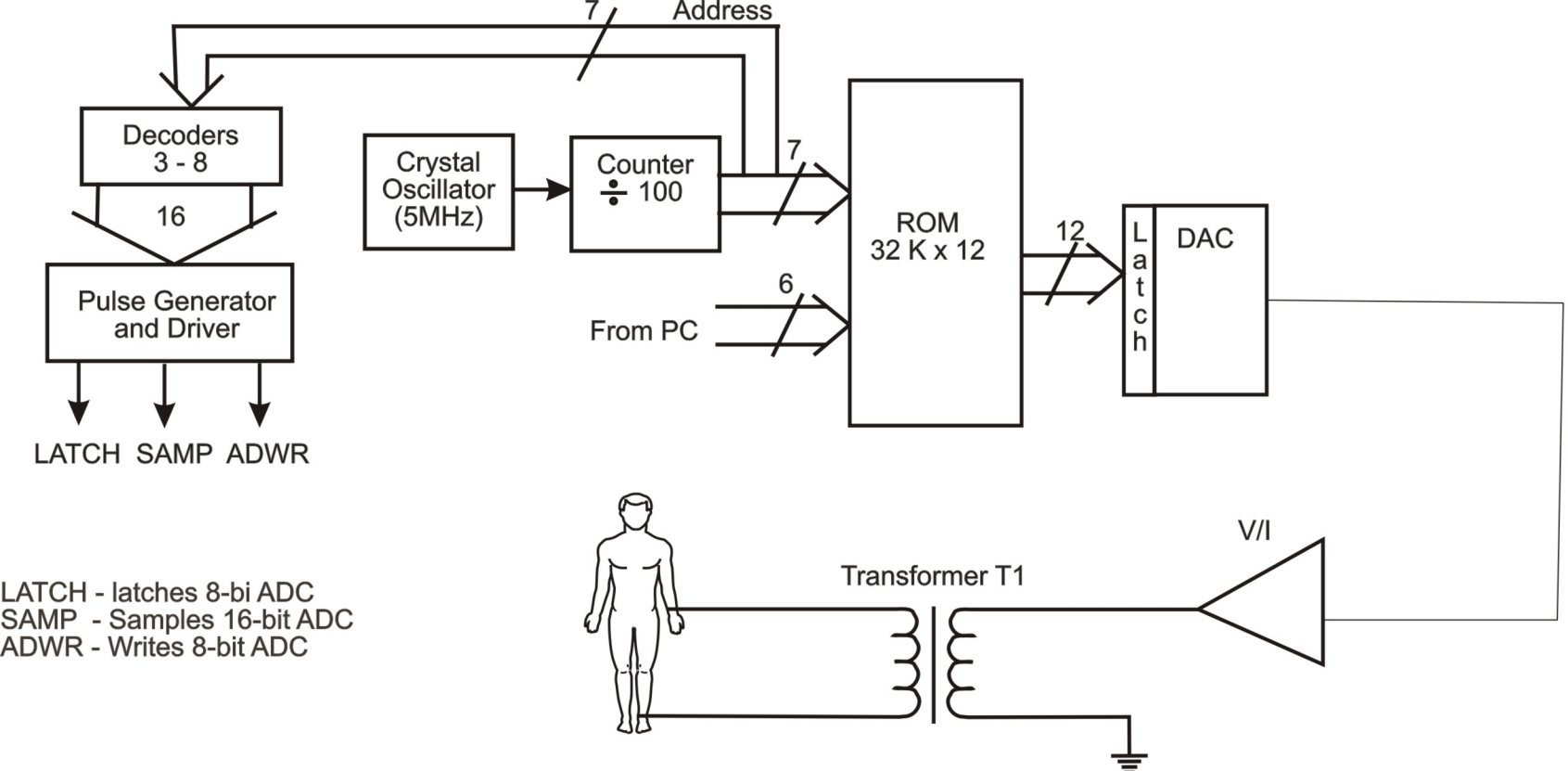

Figure 3: Block Diagram of the Constant Current Source

Table 1: Specifications of the Present System

Parameter	Value(s)
Number of Measurement channels	3
Current source signal	10 mA p-p, 50 kHz
ΔZ sensitivity	1.95 mV/mΩ (12.75 digit count/mΩ)
ΔZ frequency response	0 to 100 Hz
Z readout range	0 to 30 Ω
ΔZ noise at output	0.45 mΩ (pp) to 0.80 mΩ (p-p) * 6 to 11 digit count
ΔZ readout range	0 to 600 mΩ
ΔZ resolution	0.078 mΩ (1 digit count)
Z adjustment range of phase shift	–43.2° to 10.8°
Minimum phase shift adjustment	3.6°

* We obtain an average pulse typically based on 3 impedance pulses. The ΔZ noise in the averaged signal is around 0.26 mΩ (p-p) to 0.46 mΩ (p-p)